

On Surface Topography and Microstructure in Cavitation Erosion Tests of Alloy 80 A

C Belin*, I Mitelea, I Bordeasu and C Craciunescu

„Politehnica“ University of Timisoara, Timisoara, Romania, EU

*Corresponding author: cosmin.belin@student.upt.ro

Abstract. From practical and economic reasons for the design of components for Diesel engines, the selection of materials and /or heat treatments is essential to provide a high cavitation erosion resistance. This paper studies cavitation behavior of the Nimonic 80A alloy designed for execution of Diesel engine exhaust valves. The cavitation tests were done on an ASTM G32 -2010 compliant vibrating device with piezoceramic crystals.

The metallographic examinations performed with optical microscope and electronic scanning microscopy revealed the microstructural changes occurring in the region of the cavitation affected material and the path of the crack propagation

1. Introduction

The phenomenon of cavitation consists of the formation of bubbles/cavities filled with gases and vapors in a liquid as a result of the local pressure decrease below the vapor pressure, known as the critical value. When these bubbles come in contact with high local pressure, they will implode and generate microjets and/or shock waves [1], [2], [3]. If bubble implosion occurs near a solid surface, the microjet or shock waves create high pressure on the solid surface. When repeating such events, the surface area under such stress will suffer a local fatigue phenomenon, accompanied by elasto-plastic deformations leading to fracture, with solid material losses [4], [5]. This effect is known as cavitation erosion and is manifested in many engineering components such as hydraulic turbines and pumps, marine and river propellers, aerospace vessels, exhaust valves and combustion chambers of Diesel engines, etc. Frequently the phenomenon occurs in the parts exposed to fluids with high velocity, but also to those that vibrate in static liquids [2]. Studies in this field show that cavitation erosion can be countered by applying thermal treatments [6] to improve the mechanical properties of metallic materials or by various surface hardening techniques.

This paper highlights the cavitation erosion performance of the Nimonic 80 A alloy which has been subjected to solution quenching.

2. Experimental procedure

The considered alloy, Nimonic 80 A (EN NiCr20TiAl, UNS No. 7080, W. No. 24952 & 24631), is part of the deformable material category with high mechanical strength up to service temperatures of 815 °C [3], [4]. Vacuum refinements are commonly used in the manufacture of exhaust valves of Diesel engines and gas turbine components (vane, rotors, discs) [5]. The chemical composition of the investigated material is: 20.5% Cr, 1.98% Ti, 1.54% Al, 2.14% Fe, 1.61% Co, 0.63% Mn, 0.48% Si 0.12% Cu 0.08% % Zr, and % Ni balance. Cavitation samples were made from cylindrical rolled bars,



Ø20 x 300 mm, which were thermally treated by solution quenching, at 1080 °C for 8h and air cooled, having the shape and dimensions shown in Figure 1.

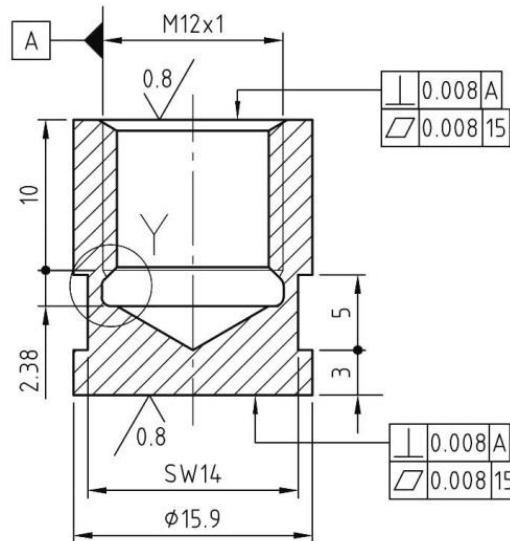


Figure 1. Cavitation sample.

Cavitation tests were performed on a vibrator device with piezoceramic crystals, which complies with the ASTM G32-2010 standard requirements (see figure 2) [6]. The functional parameters which determine the cavitation erosion intensity are: vibration amplitude of 50 μm peak-to-peak, 20000 \pm 2% Hz frequency and 22 °C \pm 1°C cavitating liquid temperature (double distilled water). To determine the wear rate through cavitation erosion, the test was interrupted at regular intervals; the samples were washed in acetone, dried in a hot air stream and weighed with an analytical balance that can weigh with an accuracy of five decimals.

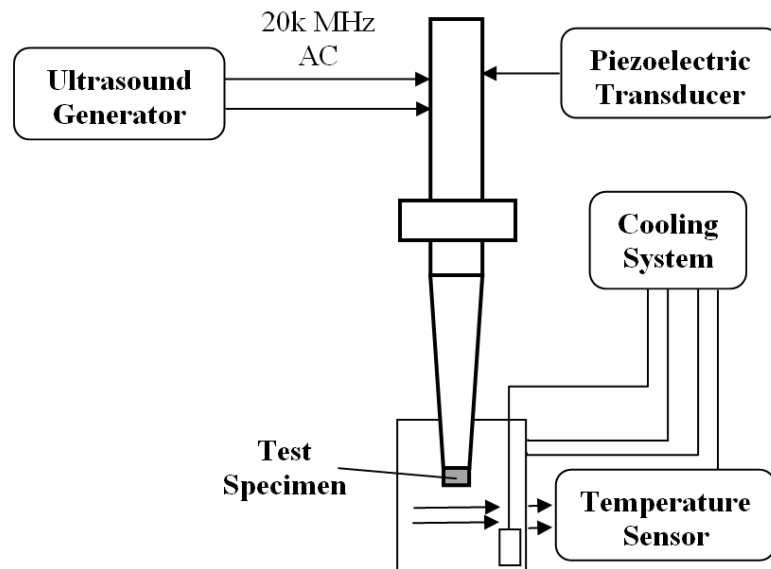


Figure 2. The ultrasonic equipment used in the cavitation erosion experiments.

The surface topography of cavitation tested samples was investigated by scanning electron microscopy.

3. Results and discussions

The microstructure obtained after the heat treatment is composed of γ solid solution grains of polyhedral form, some of which have annealing twins. Within the grains and on the separation boundaries there are secondary phase particles [3].

In Figure 3 are presented the characteristic cavitation erosion curves for the Nimonic 80 A alloy which was solution quenched at 1080°C, for 8h and cooled in air. They indicate the variation of the mass losses and their velocity, respectively the variation of the average penetration depth of the erosion and its velocity, with the duration of the cavitation attack generated by the vibratory apparatus.

The specific curves represent the cumulative mass loss ($m(t)$), the mean depth of erosion ($MDE(t)$), the specific velocities ($v(t)$) and the mean depth erosion rate ($MDER(t)$), and have the following forms [1] [2]:

$$m(t) = A1 \cdot t \cdot (1 - e^{-B1t}) \quad \text{or} \quad MDE(t) = A2 \cdot t \cdot (1 - e^{-B2t}) \quad [1]$$

$$v(t) = \frac{dm}{dt} = A1 \cdot [1 - e^{-B1t}] + A1 \cdot t \cdot B1 \cdot e^{-B1t}$$

respectively

$$MDER(t) = \frac{dMDE}{dt} = A2 \cdot [1 - e^{-B2t}] + A2 \cdot t \cdot B2 \cdot e^{-B2t} \quad [2]$$

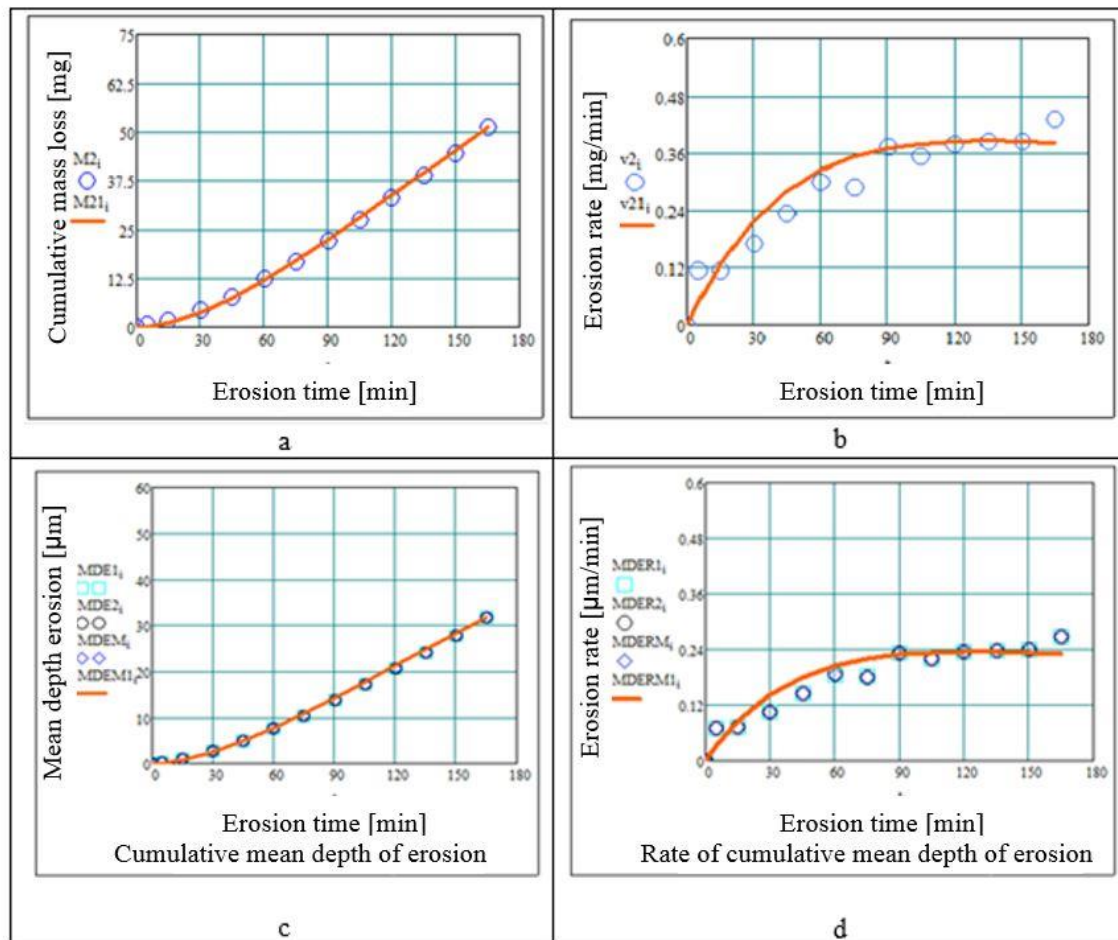


Figure 3. Characteristic cavitation erosion curves for the Nimonic alloy
a - Cumulative mass losses [mg]; b - Erosion rate [mg/min]; c - Mean depth of erosion, MDE [μm]; d - Mean depth erosion rate, MDER [$\mu\text{m}/\text{min}$].

The form of the approximation curves of the experimental points, as well as the dispersions of the points against these curves, (fig. 3), demonstrate the following:

- a small degree of dispersion of the experimental points compared to the approximation curves, specific to the materials with a good resistance to cavitation erosion due to high mechanical resistance characteristics;
- roughly linear variations of the curves $m(t)$, Figure 3a, MDE (t), Figure 3 c respectively, after about 90 minutes of cavitation exposure, which results in the stabilization of the erosion rate to the maximum value ($\cong 0.39$ mg /min, respectively $\cong 0.24$ $\mu\text{m}/\text{min}$), phenomenon encountered only in materials with increased cavitation resistance.

The images shown in Figure 4. obtained with the Canon Power Shot A480 camera, the resolution of which, furthermore, highlights the extent of surface degradation and less in depth at various times of the cavitation attack, shows the evolution of surface degradation as a function of the resistance provided by the thermal treatment applied. These images (Fig. 4) represent the values and dispersions of the experiments points versus the erosion speed curves in Fig. 3b and 3d. Thus, it can be seen that:

- During the 5 minute-10 minutes of vibratory cavitation (the first two experimental points), the erosion speeds have very close values, reflected by craters and ring formation from the periphery of the cavitated surface. During these periods, the roughness peaks resulting from the mechanical grinding and abrasive dust remaining after the washing are eliminated before the actual test begins;
- after this attack time, up to 60 minutes (inclusive) the erosion rate increases, which leads to the extension of the degradation on the entire exposed surface;
- Within 60-75 minutes, the erosion rate has a slight decrease due to the compressing cavitation layer. By its repetitive impact with microjets and shock waves generated by the implosions of cavitation bubbles, stellar caverns are starting to form at the periphery of the surface due to the expulsion of grains, which bonds were cracked by the impact force between the microjets and the exposed surface;
- in the interval of 90-150 minutes, the erosive process is carried out at close speeds values due to the behavior of the layer, which, beyond a natural hardening by cold deformation, provides a constant attenuation of the impact force through the air pockets that penetrate the microcracks, blocking the propagation of cracks across the whole area / with large expulsions of material, but emphasizing the growth of caverns from the peripheral area;
- local fatigue takes place during the last cavitation period (150-165 minutes), when the speed has a jump (the last experimental point) as a result of the expulsion of a larger amount of material generated by the crack network formed earlier, which, uniting, leads to the fracture of boundaries, but also within the grains interior.

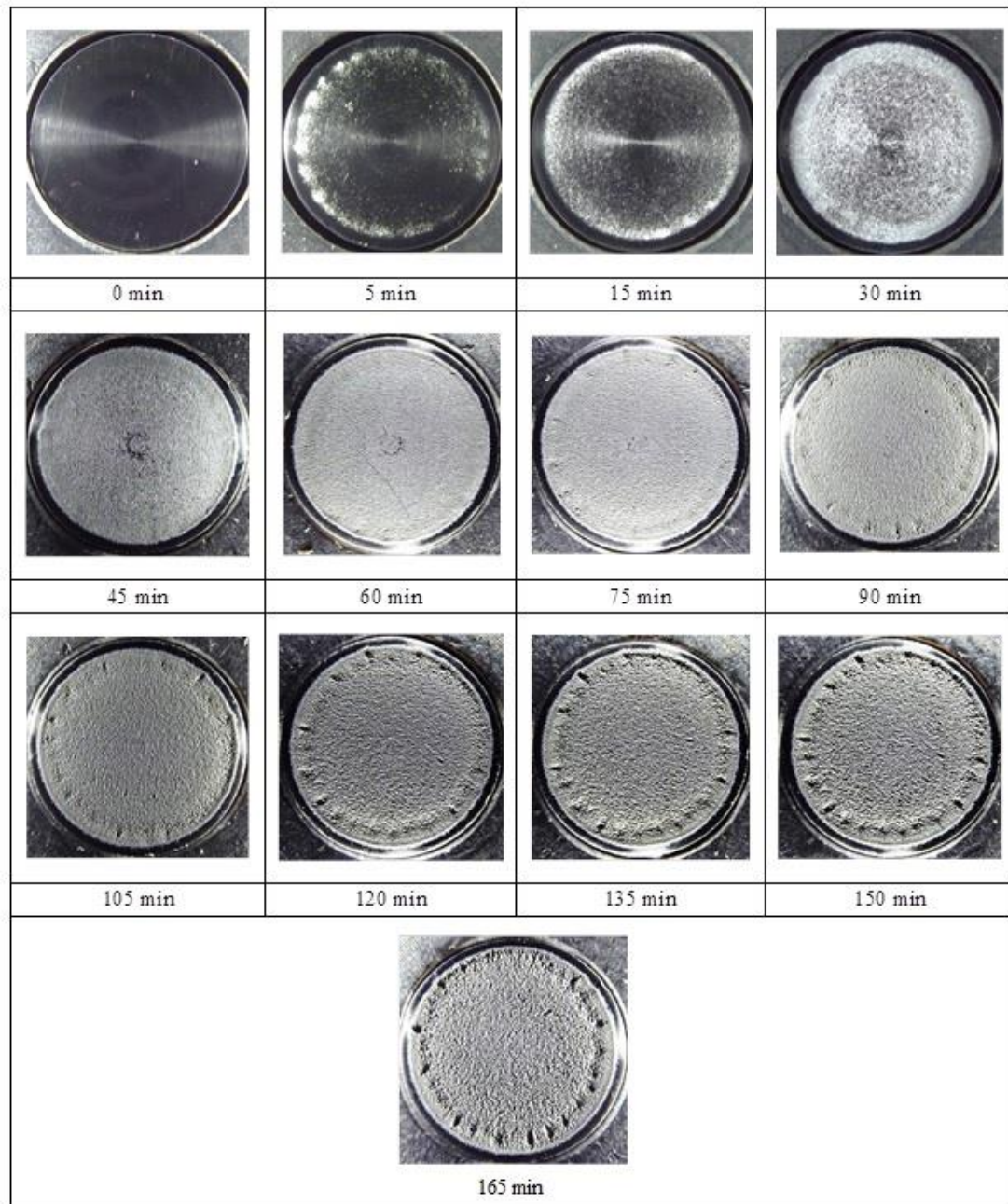


Figure 4. Aspect of the surface of samples tested at cavitation.

The statistical processing of the experimental results, with the determination of the tolerance interval in which the experimental point's dispersion fall (Figure 5.), demonstrates the accuracy of the measurements performed. The upper and lower limits of the dispersion band were constructed according to the procedure described in [1], using the standard estimation error σ and the exponential regression curve of the form (1), which approximates the experimental values of the three tested samples.

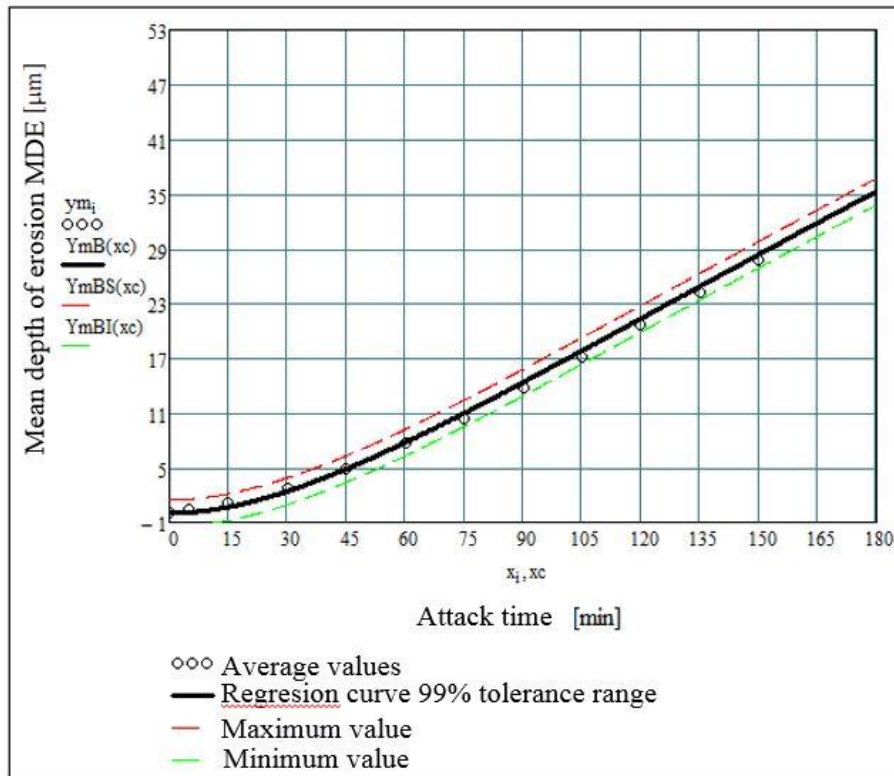


Figure 5. Sample dispersion band tested at cavitation.

The 99% tolerance range shows the low dispersion band and the uniform surface behavior of the cavitation attack. In fact, it is a reflection of the homogeneous distribution of mechanical properties (hardness, tensile strength, yield strength, toughness) that define the cavitation resistance of the material [2], [6]. The small differences in the error band are natural due to the complexity of the cavitation erosion process.

Figure 6 illustrates the topography of the samples tested at ultrasonic cavitation for 165 minutes. It is observed that the removal of material particles is uniform, being characteristic of the f.c.c. crystalline network (face-centered cubic), and that some differences in cavity depths occur.

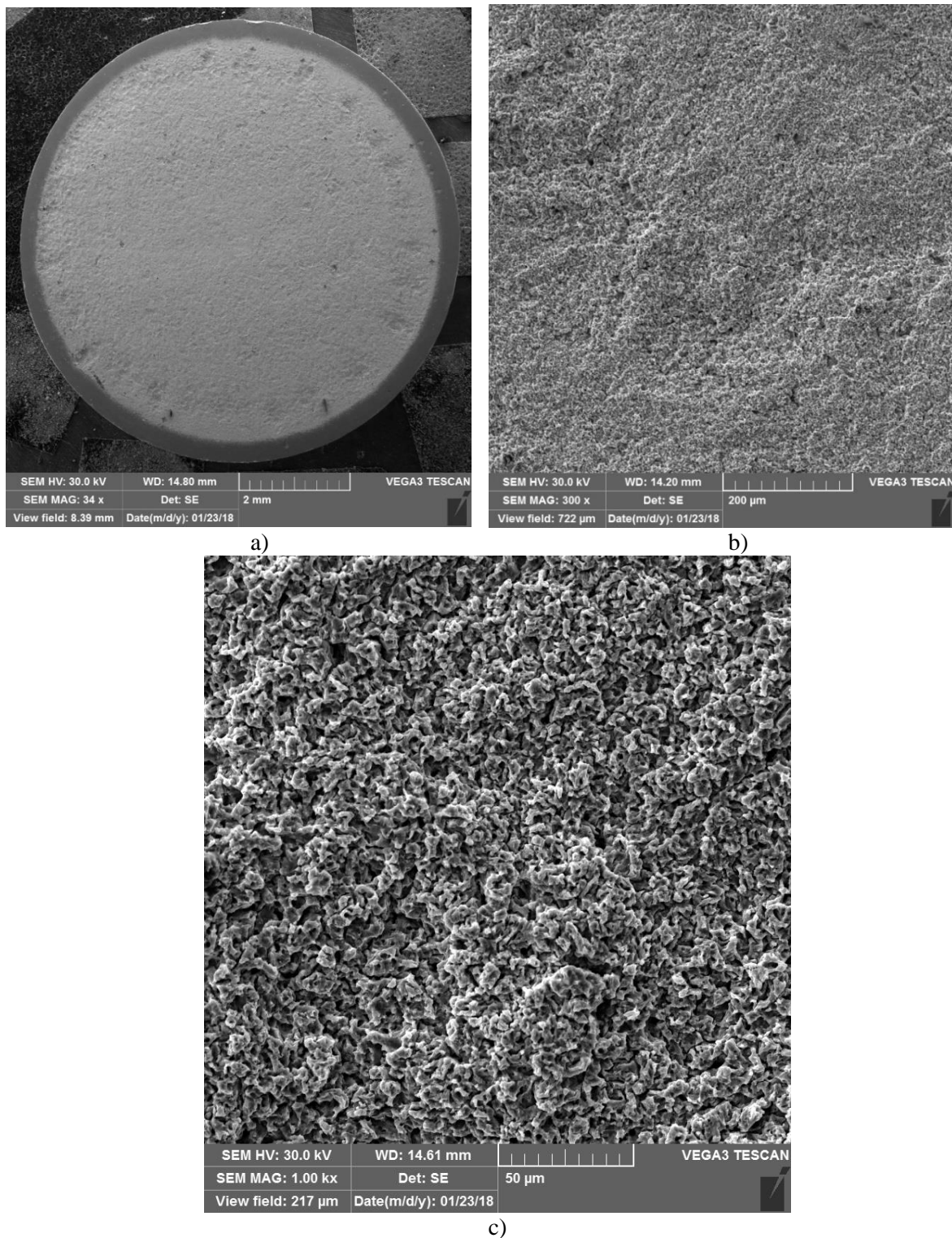


Figure 6. Macro (a) and micrograph images (b, c) of the cavitation exposed surface for 165 min. after solution treatment.

The formed cavities were initiated on the crystalline grains boundaries, where there are phases of chemical combinations, and as the erosion progresses, the attack occurs in the γ solid solution matrix.

4. Conclusions

The cavitation behaviour of the investigated material is characteristic to the alloys with an austenitic microstructure with a f.c.c. crystalline network and secondary phases placed inside and on the grain boundaries.

For the experimental conditions used, after 165 min. of cavitation attack, the mean depth of erosion, MDE, is about 32 μm and the mean depth erosion rate, MDER, tends to stabilize at 0.24 $\mu\text{m} / \text{min}$.

The shape of the erosion speed curves, with maximum capping, and the low degree of dispersion of the experimental points from them, show that the studied Nimonic alloy has a good behavior in the vibrational cavitation erosion, specific to the materials with high mechanical characteristics.

The analysis of surface degradation over various cavitation times (Fig.4), correlated with the experimental values of the erosion speeds (Fig.3b and 3d), allowed the description of the damage mechanism, which occurs due to the impact between the samples surface and the shock waves, respectively by the microjets resulted from the implosion of cavitation bubbles.

The surface wear phenomena are triggered on the grain boundaries and advances into the γ solid solution matrix.

5. References

- [1] Bordeasu I, Patrascoiu C, Badarau R, Sucitu L, Popoviciu M and Balasoiu 2006 *FME Transactions Faculty of Mechanical Engineering, New Series* **34(1)** 39
- [2] Bordeasu I 2006 *Eroziunea cavitațională a materialelor* (Editura Politehnica, Timișoara)
- [3] Baumgaertner T, Plath A, Kempf B, Bothe K and Gerold V 1989 *Strength of Metals and Alloys (ICSMA 8)* **3** 1045
- [4] Matthew DM, Singh V, Chen W and Wahi PR 1991 *Acta Metallurgica et Materialia* **39(7)** 1507
- [5] Di Martino FS, Faulkner GR, Hogg CS, Vujic S and Tassa O 2014 *Materials Science & Engineering A* **619** 77
- [6] Mitelea I, Bordeasu I, Katona SE and Craciunescu CM 2017 *International Journal of Materials Research* **108(12)** 1099